Kingdom of Saudi Arabia

Imam Mohammad bin Saud

Islamic University College of

Science

Chemistry Department

Kinetic investigation of ciprofloxacin adsorption onto carbon nanoparticles prepared from waste materials

Research submitted as partial fulfillment of the requirements for the completion of the BSc Degree in Chemistry

By

Suliman Ziad Suliman Al-musallam (441016166)

&

Abdulaziz maged abdulaziz alnafea (441016901)

Supervisor

Dr. Faisal Khuwayshan Algethami

May 2024

Acknowledgement & Dedication

We express our heartfelt gratitude to our supervisor, Dr. Faisal Algethami, for his excellent leadership.

Also, we express our gratitude to the chemistry teaching team for their efforts.

We dedicate this work to our families for their ongoing support and encouragement.

No.	Contents	Page No.
	The objective of the study	5
	Arabic abstract	6
	English abstract	7
	Chapter 1 General introduction and literature review	
1.	**Introduction and literature review**	8
1.1	**Sources of water pollution**	8
1.2.	**Occurrence of water pollutants**	10
1.3.	**Preparation and uses of nanomaterials**	14
1.4.	**Water treatment**	15
1.5	**Adsorption**	18
1.6	**Aim of the study**	19
	Chapter 2 Materials and methods	
2	**Materials and Methods**	21
2.1	**Materials**	21
2.2	**Adsorption of CFXN**	21
	Chapter 3 Results and discussion	
3.	**Results and discussion**	23
3.1	**Adsorption of CFXN**	23
3.2	**Adsorption Rate Order study**	25
3.3	**Mechanism controling SFXN adsorption**	29
3.4	**Conclusion**	32
	Reference	33

الملخص باللغة العربية

يعد تلوث المياه بالمواد الصيدلانية من خلال تصريف مياه الصرف الصناعي مشكلة بيئية عالمية. نتيجة لذلك ، أدخل العديد من الباحثين طرقًا مختلفة لمعالجة مياه الصرف الدوائية. في هذه الدراسة ، تم استخدام **جسيمات** الكربون النانوية المصنعة من بذور الزيتون (OCNP) ، قشرة القهوة (CCNP) ، وقشور الفول السوداني (PCNP) للتخلص من السيبروفلوكساسين من الوسط المائي. أوضحت النتيجة التي تم الحصول عليها أن قيم سعة الامتصاص القصوى لـ CCNP و OCNP و PCNP كانت 194.86 مجم جم -1 ، 121.21 مجم جم -1 ، و 51.21 مجم جم-1 على التوالي. تم تحقيق حالات التوازن لـ PCNP و CCNP في غضون 45 دقيقة ، بينما تم الوصول إلى حالة التوازن لـ OCNP بعد 90 دقيقة. بناءً على نتائج الدراسة ، وجد أن حركية امتصاص سيبروفلوكساسين على CCNP و OCNP و PCNP تتبع النموذج الحركي من الدرجة الثانية الزائفة (PSO) . علاوة على ذلك ، أظهرت التحقيقات الخاصة بآلية التحكم في معدل الامتصاص أن نموذج انتشار الفيلم السائل يتحكم في امتزاز السيبروفلوكساسين (CIP) على CCNP و OCNP و PCNP.

Abstract

Contamination of water by pharmaceutical substances through the discharge of industrial wastewater is a world wide environmental problem. As a result, many researchers have introduced various methods for treating pharmaceutical wastewater. In this study, a carbon nanotube synthesized from olive seeds (OCNP), coffee skin (CCNP), and peanut shells (PCNP) was used to eliminate ciprofloxacin from aquatic media. The obtained result revealed that the maximum adsorption capacity values for CCNP, OCNP, and PCNP were 194.86 mg g-1, 121.21 mg g-1, and 51.21 mg g-1, respectively. The equilibrium states of PCNP and CCNP were achieved within 45 minutes, while the equilibrium state of OCNP was attained after 90 minutes. Based on the study results, it was found that the adsorption kinetics of Ciprofloxacin on CCNP, OCNP, and PCNP followed the The pseudo-second order kinetic model (PSO). Furthermore, the investigations of adsorption rate control mechanism showed that the liquid-film-diffusion model controlled the ciprofloxacin (CIP) adsorption on CCNP, OCNP, and PCNP.

Chapter I
Introduction

1. Introduction and literature review

To put it simply, water pollution occurs when substances that should not be in the water are there, damage the quality of the water, or pose threats to living beings [1, 2]. The importance of water to human survival cannot be overstated. Despite its seeming abundance, only a fraction of this renewable resource is usable at any given time. In addition, many of the world's water sources are polluted, and they are distributed unequally. Water scarcity affects millions of people worldwide, contributing to numerous wars [1]. River baseflow relies heavily on groundwater, which can be brought to the surface through springs or collected through excavation or drilling [2]. There has been a dramatic increase in water pollution and wildlife contamination in recent years, leading to a deficit in water for human use and agricultural irrigation. After contaminated water supplies were introduced, waterborne infections have repeatedly wiped out entire city populations [3]. About 80% of marine environmental contaminants originate on land, either directly from industrial processes or indirectly through the disposal of diverse residues arising from human activities [4]

1.1. Sources of water pollution

a. Sewage and wastewater

Water that has been used is referred to as wastewater. It is produced by commercial, industrial, and agricultural activity and by our sinks, showers, and toilets. Stormwater runoff transports road salts, oil, grease, chemicals, and debris from impermeable surfaces into our rivers. According to the UN, over 80% of

the world's wastewater is dumped into the environment untreated; in some countries, the figure is as high as 95%. In the United States, wastewater treatment plants treat around 34 billion gallons daily. These facilities reduce impurities such as pathogens, phosphorus, nitrogen compounds, heavy metals, and toxic chemicals before reintroducing treated waters into rivers.

b. Oil pollution

Although massive spills make headlines, the majority of oil pollution in our oceans is caused by consumers, including oil and gasoline that seeps from millions of automobiles and trucks daily. Furthermore, nearly half of the estimated oil spilled into the sea comes from land-based sources such as factories, farms, and towns rather than tanker accidents. Tanker spills account for around 10% of the oil in the world's waterways. Simultaneously, the maritime industry's everyday operations contribute roughly one-third.

c. Chemical pollution

Industrial chemical waste can only be processed in special treatment plants; sewage treatment plants cannot handle them. Water contaminants can infiltrate the aquatic environment from various sources, including mines, manufacturing effluents, and light industry, as well as roof runoff in areas where metal roofing is a potential culprit. Domestic effluent that has either been bypassed or poorly treated, road runoff including abraded tier, brake, and engine material and lead from exhaust emissions in regions where lead had not previously been exposed have all been removed from gasoline. Cadmium, chromium, arsenic, mercury,

lead, copper, zinc, and nickel have been identified as priority control pollutants by the US Environmental Protection Agency due to their high toxicity. They are on the WFD list of substances that should be minimized or phased out in Europe. Cadmium, mercury, and lead emissions from all sources have steadily reduced throughout Europe since 1990. Agricultural chemicals prone to enter the aquatic environment include fertilizers, pesticides, and metal salts such as copper sulfate. Historically, crops were fertilized using animal waste and plant-based materials such as compost or rotting seaweed, followed by guano, nitrate, and phosphorus. Excessive nitrates, typically found in private wells, can cause 'blue baby syndrome' and methemoglobinemia in nitrate-hypersensitive babies.

1.2. Occurrence of water pollutants

An extensive monitoring effort across the Netherlands between 2010 and 2014 revealed alarmingly high pesticide concentrations in groundwater wells. Studying groundwater from 127 locations, the researchers analyzed 90 samples. The analysis of these samples for 405 pesticides and 52 metabolites in the Netherlands and Flanders region revealed the presence of highly mobile and persistent neonicotinoids in shallow groundwater samples, with concentrations ranging from 0.12 g/L to 0.01 g/L [5]. The levels of organochlorine and organophosphate insecticides in the Yangtze River Basin (Hubei Province, Central China) were much above safe levels for human consumption [6]. Fifteen organochlorine pesticides and four organophosphate pesticides were detected in sixteen groundwater samples taken from this area. Aldrin, dieldrin,

hexachlorocyclohexane, and 196.01 ng/L were the average concentrations of the four organophosphate pesticides measured in the study. U.S. Environmental Protection Agency's drinking water standards were broken (US EPA) [7]. Detection of organochlorine pesticides in the phreatic aquifer beneath the Pampean region of Argentina suggests that these chemicals can persist for a considerable amount of time in the subterranean water table [8].

Numerous investigations have demonstrated elevated groundwater fluoride levels in a number of locations. Human health can be negatively affected by prolonged exposure to fluoride, which is found in groundwater. The health advantages of fluoride support the practice of fluoridating public water supplies. However, skeletal and dental fluorosis can develop if exposed to excessive quantities of fluoride. In many parts of the world, fluoride concentrations in the groundwater and soil are rather high. About 12 million tons of the world's total 85 million tons of fluoride reserves are located in India. It is not unexpected that India has a high fluoride concentration in its groundwater. Analyses of 28 samples of groundwater from hand pumps (22 samples) and tube wells in Agra City, India, revealed that fluoride concentrations in the water varied from 0.90 to 4.12 mg/L, with an average value of 1.88 mg/L. (6 samples). Of the 28 samples of groundwater examined, 64 percent had concentrations over the maximum allowed level of 1.5 mg/L. Only 32% of the samples met the WHO's standards for safe drinking water, and only 3% of the groundwater samples met the 1.0 mg/L criteria. The authors claim that excessive fluoride levels can be

traced back to natural and human-made geological processes. Chronic intake levels of exposure for infants, children, and adults were calculated to be 0.69, 0.31, and 0.12 mg kg1 d1, respectively, based on the health risk assessment results. Based on these findings, noncarcinogenic risk (dental fluorosis) appears to be greatest in infants and young children [9]. Groundwater samples from the Siddipet Vagu region of India also showed high fluoride levels. On average, fifty-one samples of local groundwater were analyzed, and their fluoride levels ranged from 0.5 to 3.7 mg/L. The fluoride levels in 51% of the samples were higher than the safe limit of 1.5 mg/L established by the World Health Organization. The fluoride concentrations in all 128 samples of groundwater from Markapur, Andhra Pradesh, India, were exactly the same. The average fluoride level was 1.98 mg/L, with a range of 0.4 to 5.8 mg/L. It was found that the amounts of fluoride in 54 out of 128 samples tested were too high [10]. Numerous studies have shown that groundwater is increasingly at risk from anthropogenic pollution. To foretell the medium and high susceptibility to groundwater pollution due to agricultural operations, the Intrinsic Groundwater Vulnerability Index was created. Approximately 62% of the area is medium vulnerable to groundwater pollution, and 38% is highly vulnerable, according to an analysis of fifty borehole samples collected from intensive agriculture on the West Bank of the Nile River in Luxor Governorate, Egypt. Over half the area was also very susceptible to nitrate pollution from intensive agriculture (52%). The authors argue that to prevent groundwater contamination, it is necessary to

optimize ongoing agricultural operations, especially using nitrogen-based fertilizers [11]. Studies have already shown a connection between agricultural activities and excessive nitrate pollution. Chungcheong Province in South Korea, for instance, has shown signs of excessive nitrate pollution, with a mean concentration of 12.4 mg/L, particularly in its agricultural regions.[12]. The indigo carmine (IGC) dye is a hazardous indigoid dye found in textile and other industries' wastewater. Dye residues have an impact on the biological processes of receiving water and obstruct light transmission, which is necessary for photosynthesis, and the commonly used approaches are ineffective for all pollutants.[13-17]. The anionic dye indigo carmine (IGC) was removed from the aqueous solution by calcined $Mg-Al-CO_3$ and was examined in batch mode. The sorption followed the Freundlich-isotherms-model The intercalation of the organic ion was also clearly demonstrated by the net increase in basal spacing for $Mg-Al-CO_3$ [18]. Surface-coated magnetite nanoparticles (Fe_3O_4-NPs) were crosslinked onto amidoxime-polyacrylonitrile (APAN) nanofibers. IGC was removed from aqueous solutions using Fe_3O_4-NPs. The pH of the solution was found to have a substantial effect on IGC adsorption. The maximum loading capacity at pH 5 was determined to be 154.5 mg/g. The Langmuir model governs indigo carmine adsorption.[19]. Electrocoagulation was used to treat wastewater containing indigo carmine dye, and a batch reactor outfitted with a mild steel anode was run under galvanostatic conditions. pH, starting concentration, current density, support electrolyte, and time are all factors. Voltage and pH

13

were measured, and the quantity of energy used was calculated precisely. The rate constant was calculated using the pseudo-first-order kinetic model [20]. By solvent sublation of the complex indigo carmine-cetyltrimethylammonium ammonium bromide (CAB) into 2-octanol, the anionic dye indigo carmine (IC, $C_{16}H_8N_2Na_2O_8S_2$) was extracted from an aqueous solution. The most efficient removal approach used a stoichiometric amount of surfactant (surfactant: dye, 1:21), which removed approximately 93 percent of the IC from the aqueous solution in about five minutes via solvent sublation [21].

1.3. Preparation and uses of nanomaterials

Co-precipitation was used to create Al_2O_3-ZrO_2 nanocomposites, which were then microwave hydrothermally treated at 270°C and 60 MPa before being calcined at 600°C. The nanomaterial Furthermore, because of decreased grain formation, the Al2O3 phase's stability was enhanced to 1200 °C, improving the sintering process [22]. A spark plasma sintering (SPS) method was used to create a porous alumina-carbon nanotubes (Al_2O_3-CNT) nanocomposite membrane for water treatment. A powder mixture of Al_2O_3 and 5 wt% CNT was generated using starch as a pore-forming agent, gum Arabic, and sodium dodecyl sulfate as dispersants. After sintering the powder mixture with SPS, a solid but porous nanocomposite membrane was formed. The membrane extracted cadmium (II) from water [23]. At ambient temperature, 1.0 g of chitosan/aluminum oxide (CS/Al_2O_3) nanocomposite film was produced by dissolving 1.0 g of CS in 50 mL of acetic acid (2 percent v/v). The CS solution's pH was adjusted to around

6.5. Under continuous stirring, 0.5 g of Al_2O_3 nanopowder suspension was added to the CS solution in double-distilled water. The mixture was agitated for another 3.0 hours at ambient temperature before being cast into a 100 mm Petri dish and dried overnight at 70°C. The resulting CS/ Al_2O_3 nanocomposite film was washed with distilled water, dried at 60°C, agitated for 3.0 h at room temperature, and then dried overnight at 70°C [24]. Al_2O_3 films were produced at room temperature utilizing various carrier gas compositions and the aerosol deposition method. The layers were applied on alumina substrates, and the film stress of each layer was determined by measuring the substrate's deformation. It has been established that using oxygen as the carrier gas rather than nitrogen or helium can cut film stress in half. The substrates were annealed at various temperature increments to learn more about how temperature influences the reduction of applied pressure. Complete tension release is already attainable at 300 °C [25].

1.4. Water treatments

Because there are so many different kinds of pollution and sources of contamination, various methods have been employed for water treatment, including sedimentation, filtration, disinfection, sludge treatment, oxidation, coagulation-precipitation, reverse osmosis, electro-dialysis, and ion exchange [26-28]. Some of the major drawbacks of these technologies include their hefty price tag and the necessity for constant monitoring [29].

1.4.1 Coagulation

The coagulation process involves combining small particles into larger aggregates and adsorbing organic matter onto particulate aggregates for subsequent solid/liquid separation. [30]. The removal of PPCPs by coagulation may be via electrical neutralization of PPCPs by positively charged metal ions, formation of organic-ion insoluble complex, and adsorption of PPCPs by aluminum sulfate [31]. Coagulation technology has clearly failed to meet people's requirements for water quality safety as pollution problems, and water quality standards have become more serious [32].

1.4.2 Sedimentation

In water treatment, sedimentation is used to reduce the amount of suspended particles before or sometimes after coagulation. In sedimentation, suspended particles in water are allowed to settle by gravity. The particles that settle out from the suspension become sediment, known as sludge in water treatment. The sedimentation ability depends on the water flow pattern through tanks (determined by tank configuration and operational parameters) and, secondly, the particle's shape, size, and interaction with the water through drag and buoyancy forces [33].

1.4.3 Filtration

Filtration is one of the core processes in water treatment. The term refers to removing suspended solids by the physical action of water flowing through a bed packed with granular media. Filtration focuses mainly on turbidity, color,

microorganisms, and particulates [34, 35]. The process can be categorized as gravity filtration and pressure filtration, with the advantage of significantly higher flow rates for the latter. Slow sand filtration was historically the first to be employed, while rapid sand filtration was later favored because of the insufficient output of the first [36].

1.4.4 Disinfection

Disinfection is essential to water treatment to keep consumers from infectious diseases by pathogenic microorganisms. Ordinary and advanced disinfection methods include chlorine, mono chloramine, chlorine dioxide, ozone, hydrogen peroxide, UV, and electrochemical treatment. Although chlorination is the most historical disinfection method, its by-products (DHPs) were considered hazardous materials [37]. As a substituent technology, mono-chloramine could maintain the original disinfection properties and lower the formation of DHPs [38]. Ozone is a strong oxidant and could inactivate microorganisms effectively but possibly generate free radicals in human bodies [39]. Electrochemical processes in chloride and chloride-free electrolytes proved to be highly efficient in disinfection, even for chlorine-resistant microorganisms [40]. Unfortunately, this method may produce strong oxidants during electrolysis [41].

1.4.5. photodegradation

The photocatalytic process is heterogeneous catalysis bringing a light-absorbing catalyst into contact with the desired reactants in a solution or gas phase. Advantages over conventional wastewater treatment methods exist for using a

heterogeneous approach, which has been utilized successfully to decompose a wide range of harmful substances, including air and aquatic organic contaminants. For instance, active photocatalysts may only take a few hours to degrade organic pollutants at room temperature completely. Organic contaminants can be fully mineralized to non-toxic products (CO and water) without giving rise to subsequent dangerous chemicals [42].

1.5. Adsorption

Adsorption is the mass transfer of substances between two phases: liquid-liquid, liquid-solid, gas-liquid, or gas-solid. Intermolecular forces are used to adsorb any specific pollutant (adsorbate) from wastewater. The interactions between the solid surface and adsorbates are known as physisorption and chemisorption. The process is known as physisorption if the interaction has a weak physical nature, such as van der Waals forces, and the process results are reversible. It also occurs at temperatures below or near the critical temperature of the adsorbate. Chemisorption, as opposed to physisorption, involves a chemical bond between the solid surface and the adsorbates. However, it only exists as a monolayer, and adsorbates are almost always removed due to the intense contact. Both processes can occur concurrently or alternatively, depending on the circumstances. While researching adsorption methods, consider the following factors: I surface area, (ii) nature and starting concentration of adsorbate, (iii) solution pH, (iv) temperature, (v) interfering compounds, and (vi) nature and dose of adsorbent [8].

1.6. Aim of the study

This study aims to prepare carbo nanoparticles from agricultural waste as low-cost sorbents. The efficiency of the prepared nanomaterials will be studied for eliminating pharmaceutical contaminants from water. The CFXN drug will be used as a model water pharmaceutical pollutant. The kinetic of CFXN removal will be investigated, including the adsorption rate-order and the adsorption rate-control-mechanism.

Chapter II
Experimental
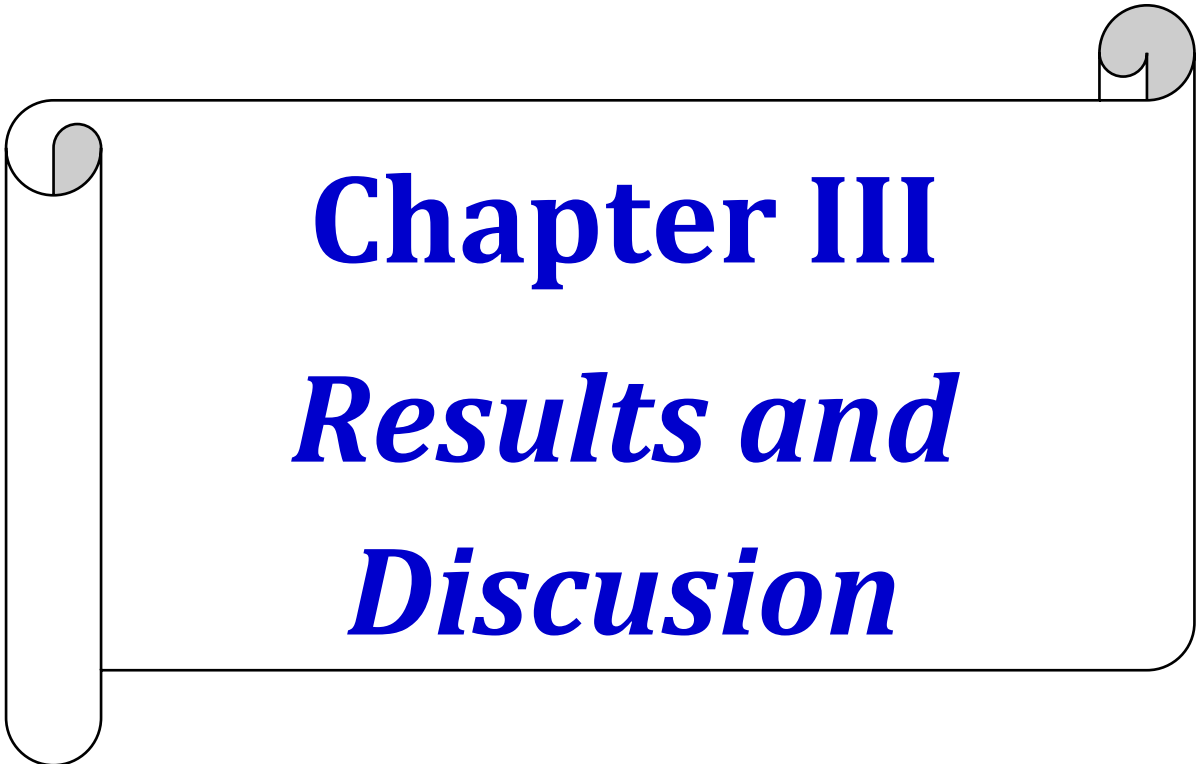
2. Materials and methods

2.1. Materials

CFXN was supplied from LOBA-CHEM, India. Carbon nanoparticles were synthesized from coffeegarlic skin (GCNPs) and peanutOlive seeds (OCNPs).

2.2. Adsorption of CFXN

A stock solution of CFXN (100 ppm) was prepared by dissolving 0.1 grams of CFXN in 1.0 L of distilled water. In a 100 mL beaker, a mass of 50 mg was measured for each sorbent. A volume of 100 mL of the CFXN solution was added to each beaker, and the mixture was stirred using a magnetic stirrer. Afterwards, 10 mL of each mixture was extracted periodically until equilibrium. In order to investigate the impact of contact time on the adsorptions of CFXN onto GCNPs and OCNPs at various time intervals, a sample was taken, filtered with a filter syringe, and measured with a UV-Vis spectrophotometer.

Chapter III
Results and Discusion

3. Results and discussion

3.1 Adsorption of CFXN

The experimental adsorption isotherms are frequently derived using an adsorbent's adsorption capacity, which is determined by the mass balance on the sorbate in a system with solution volume. Equ. 1 was used to determine the adsorption capabilities of each adsorbent for CFXN at equilibrium under the experimental conditions. Fig. 1 illustrates the impact of contact time on CFXN adsorption by GCNPs and peanut shells OCNPs. The equilibrium states of CFXN removals by GCNPs and OCNPs were achieved within 90 min, with maximum q_t values of 109.7 and 86.3 mg/g, respectively. Therefore, using CCNP shows great promise in effectively removing pharmaceutical waste due to its exceptional adsorption abilities.

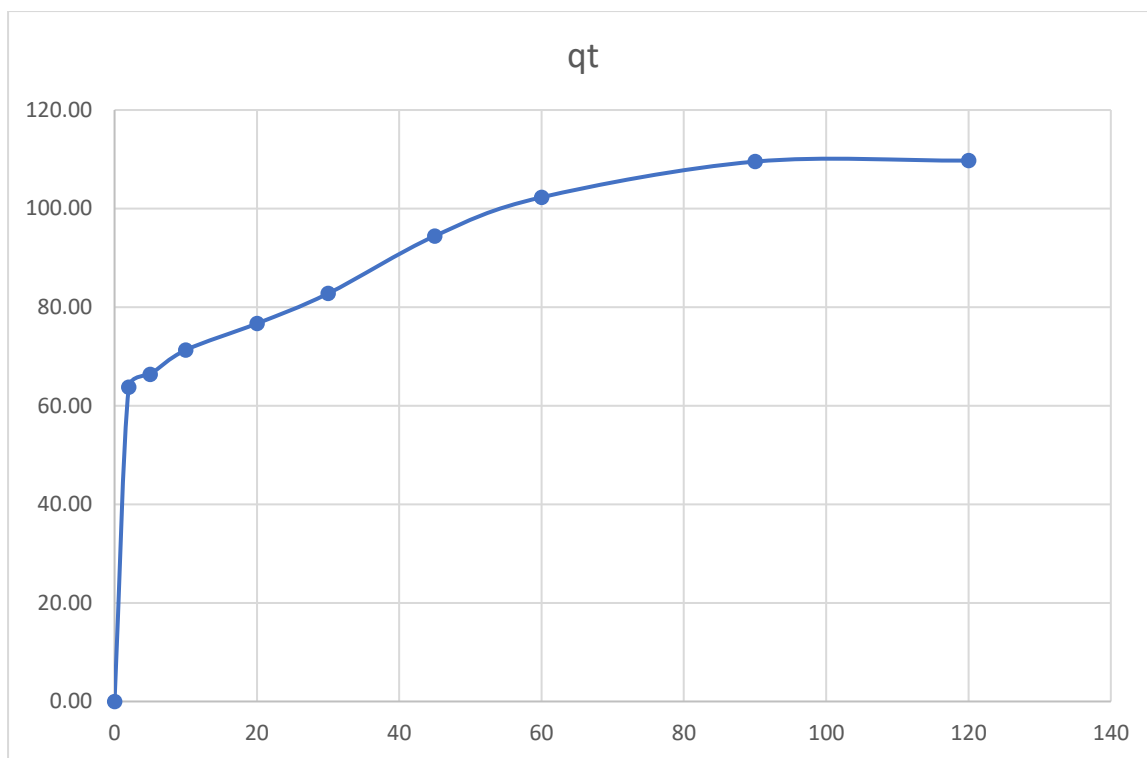$$q_t = \frac{(C_o - C_t)\, V}{m}, \qquad\qquad (1)$$

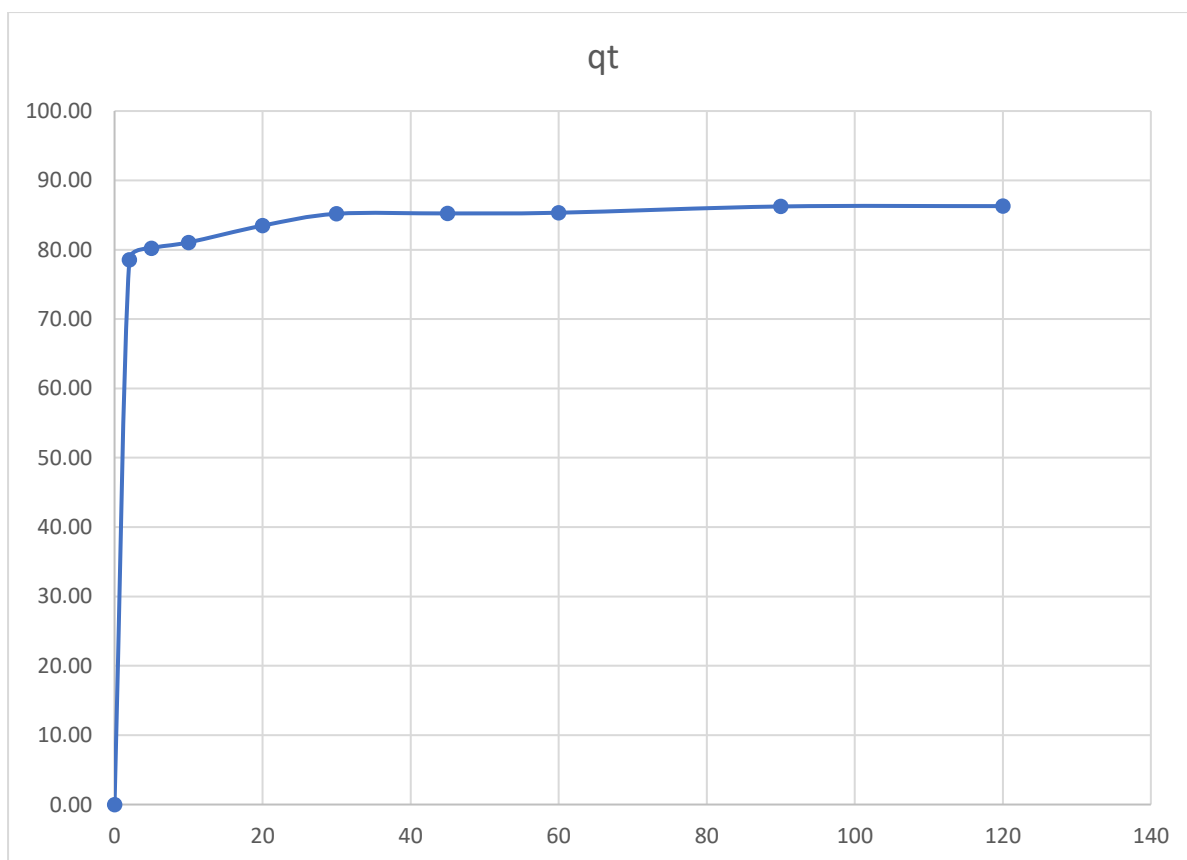Fig1: Effect of contact time on CIP adsorption by GCNPs.

Fig2: Effect of contact time on CIP adsorption by OCNPs.

Table1: Equilibrium time and Maximum adoption capacity of CCNP , OCNP and PCNP sorbents

Sorbents	Equilibrium time	Q_t (mg/g)
GCNP	90	109.7
OCNP	90	86.3

3.2. Adsorption Rate Order study

Adsorption kinetics provides insight into the reaction rate and the sorption mechanism [43]. The pseudo-first-order (PFO) and pseudo-second-order (PSO) kinetic models were employed to examine the adsorption rate of GCNPs and OCNPs sorbents. The two models are described correspondingly by formulae 2 and 3.

$$ln(q_e - q_t) = ln\, q_e - k_1.t \qquad (2)$$

$$\frac{1}{q_t} = \frac{1}{k_2.q_e^2\, t} + \frac{1}{q_e} \qquad (3)$$

Where qe (mg g1) is the adsorption capacity at equilibrium and m, v, Ct, and C o are the mass of the sorbent in grams, the volume of the solution in mL, and th e concentration of the solution in mg/L at time t (min), respectively.

The constants describing PFO and PSO are k1 (min-1) and k2 (g mg-1 min-1) respectively. Linear plots of PFO results for the adsorption of CFXN on GCNPs and OCNPs are presented in Fig. 3 and 4, while the PSO plots for removing CFXN onto GCNPs and OCNPs are displayed in Fig. 5 and 6, respectively.

Table 1 contains the obtained results for the PFO and PSO models. The PFO's correlation coefficients (R^2) were the nearest to 1. Therefore, the kinetics of CFXN adsorption onto the GCNPs, and OCNPs adsorbents can be described well by the PFO equation.
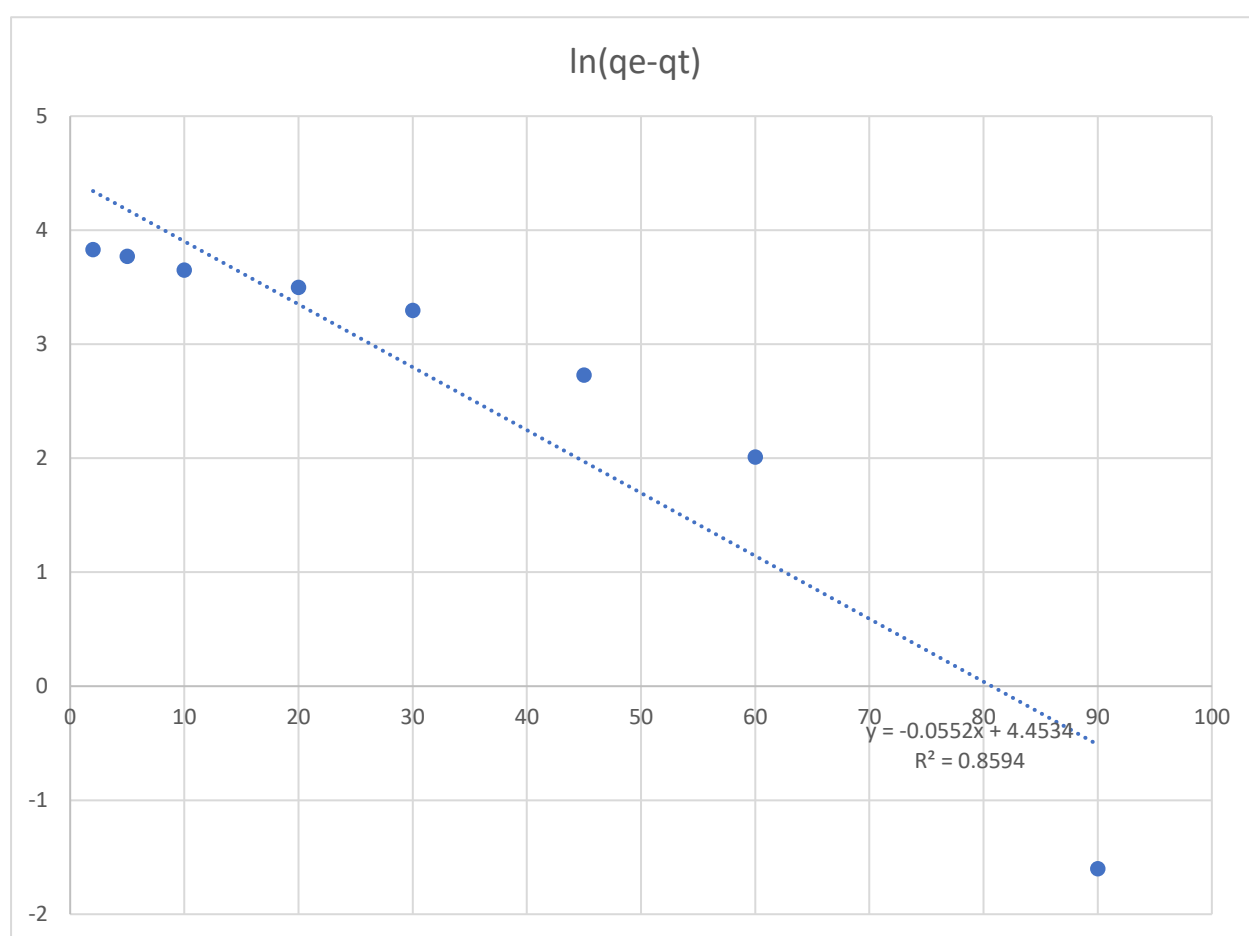

In(qe-qt)

y = -0.0552x + 4.4534
R² = 0.8594

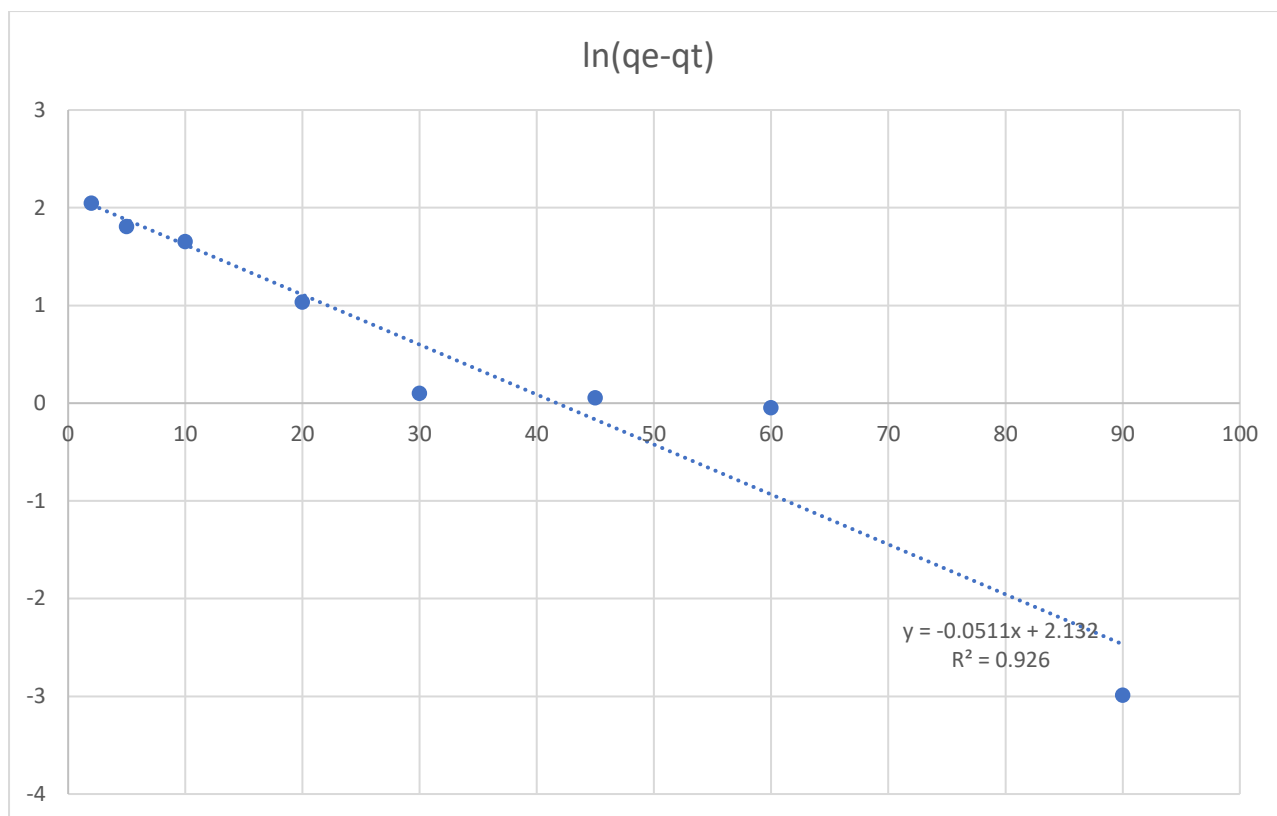Fig 3: Plot of PFO for CIP adsorption by GCNPs
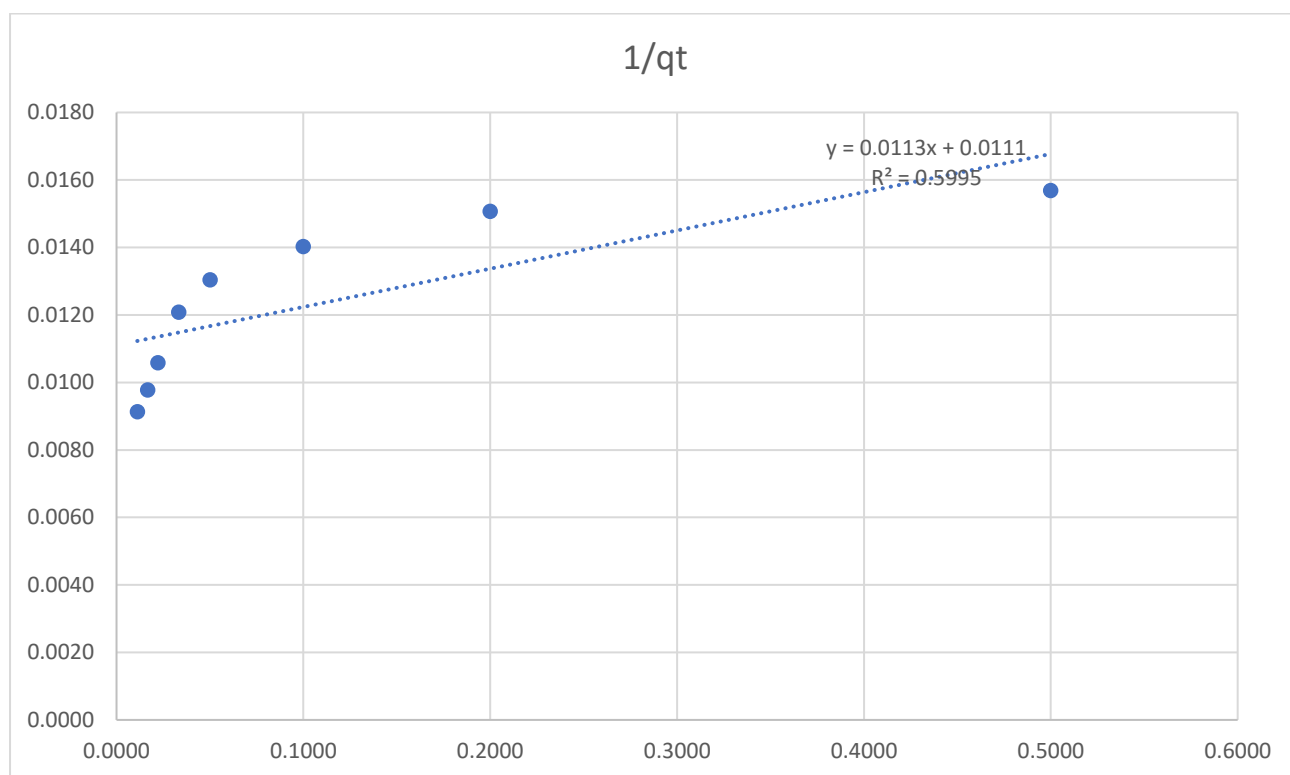
Fig 4: Plot of PFO for CIP adsorption by OCNPs

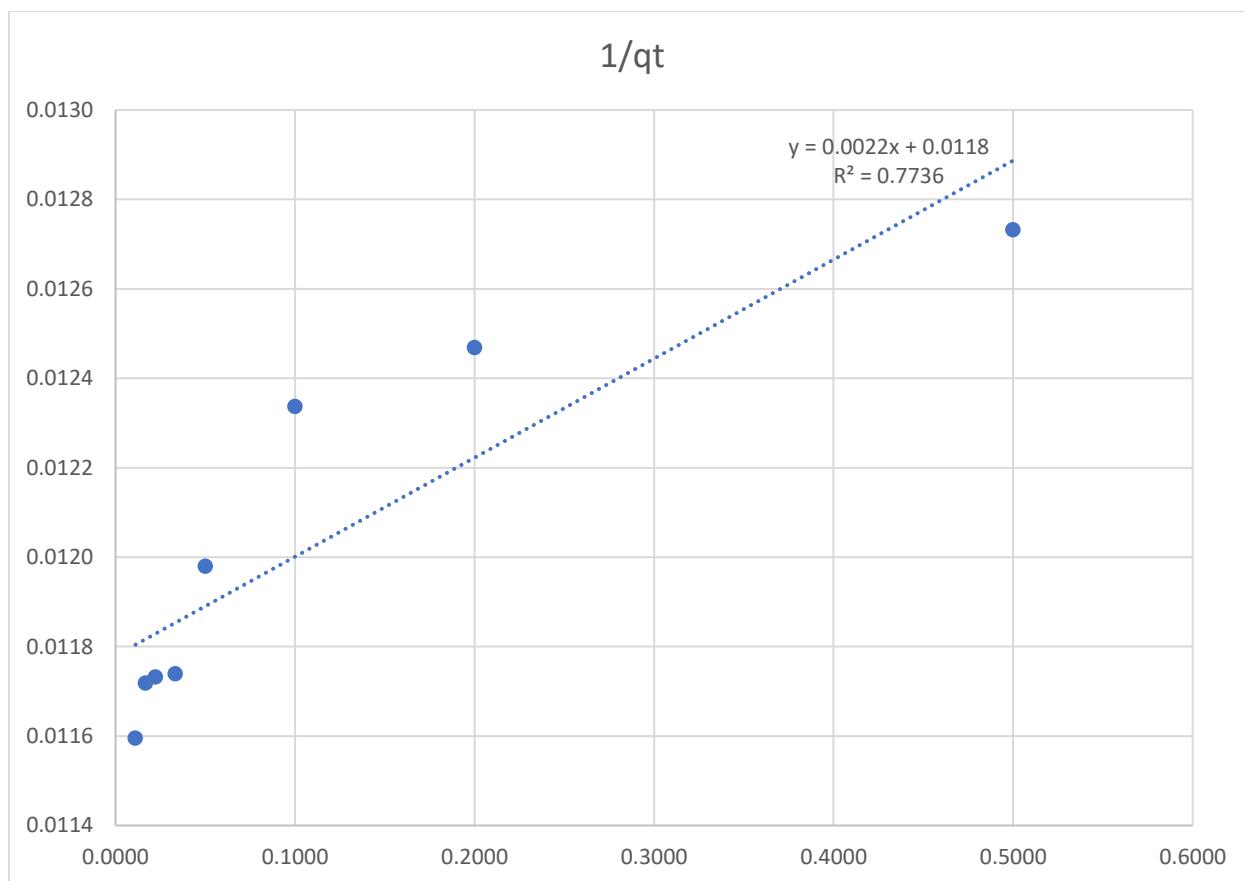Fig 5: Plot of PFO for CIP adsorption by GCNPs.

Fig 6: Plot of PSO for CIP adsorption by OCNPs.

Table 2: The adsorption rate order results for eliminating CIP using CCNP, OCNP, and PCNP.

adsorbent	q_e exp. (mg g^{-1})	PFO			PSO		
		qe cal. (mg g^{-1})	R^2	k_1	qe cal. (mg g^{-1})	R^2	k_2
GCNP	109.7	9.97	0.859	0.0632	55.92	0.600	0.0309
OCNP	86.3	33.33	0.926	0.0697	1487.44	0.774	0.0002

3.3 Mechanism controling SFXN adsorption

The adsorption process occurs in two parts. Firstly, adsorbate molecules are transferred from the liquid to the surface of the solid sorbent. Secondly, the molecules pass through the solid sorbent and into the inner layers. The rate control mechanism, also known as the slowest sorption step, regulates the adsorption rate. A study was conducted to investigate the rate-control mechanism for CFXN adsorption on CCNPs and PCNPs. The liquid-film-diffusion model (LFD, Eq. 4) and the intraparticle-diffusion model (IPD, Eq. 5) were used for this purpose [44, 45].

$$q_t = K_{IP} * t^{\frac{1}{2}} + C_i \qquad (4)$$

$$\ln(1 - F) = -K_{LF} * t \qquad (5)$$

Where: k_{ip} (mg g^{-1} min$^{-1/2}$) and k_{LF} (min^{-1}) are the IPDM, and the LFDM constants, respectively. C_i (mg g^{-1}) boundary layer factor. The linear plot for the CFXN adsorption on CCNPs and PCNPs via LFDM were monitored in Fig. 7 and 8 respectively; while the IPDM investigation was monitored in Fig. 9 and 10. The computed results for LFDM and IPDM were gathered in Table 3. The rate control mechanism obtained revealed that IPDM controlled the CFXN adsorption on the CCNPs and PCNPs.
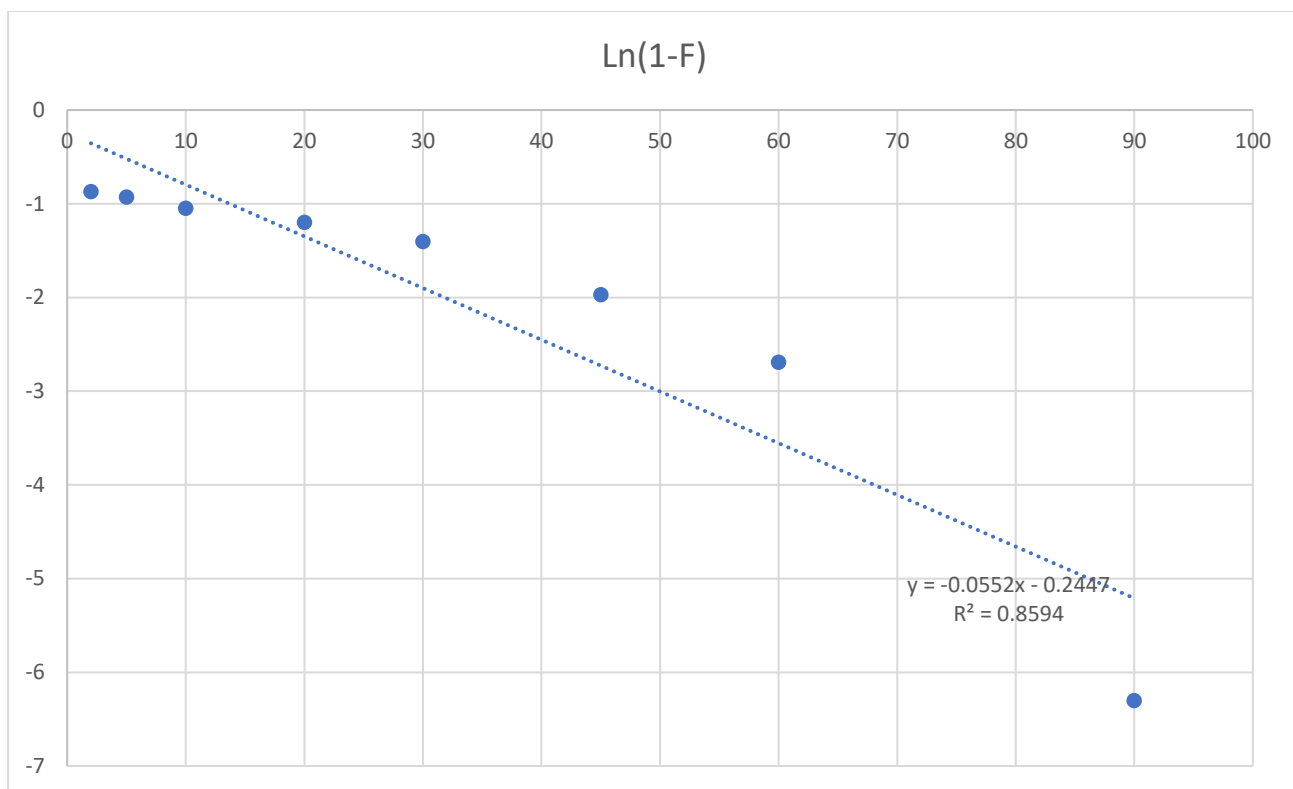
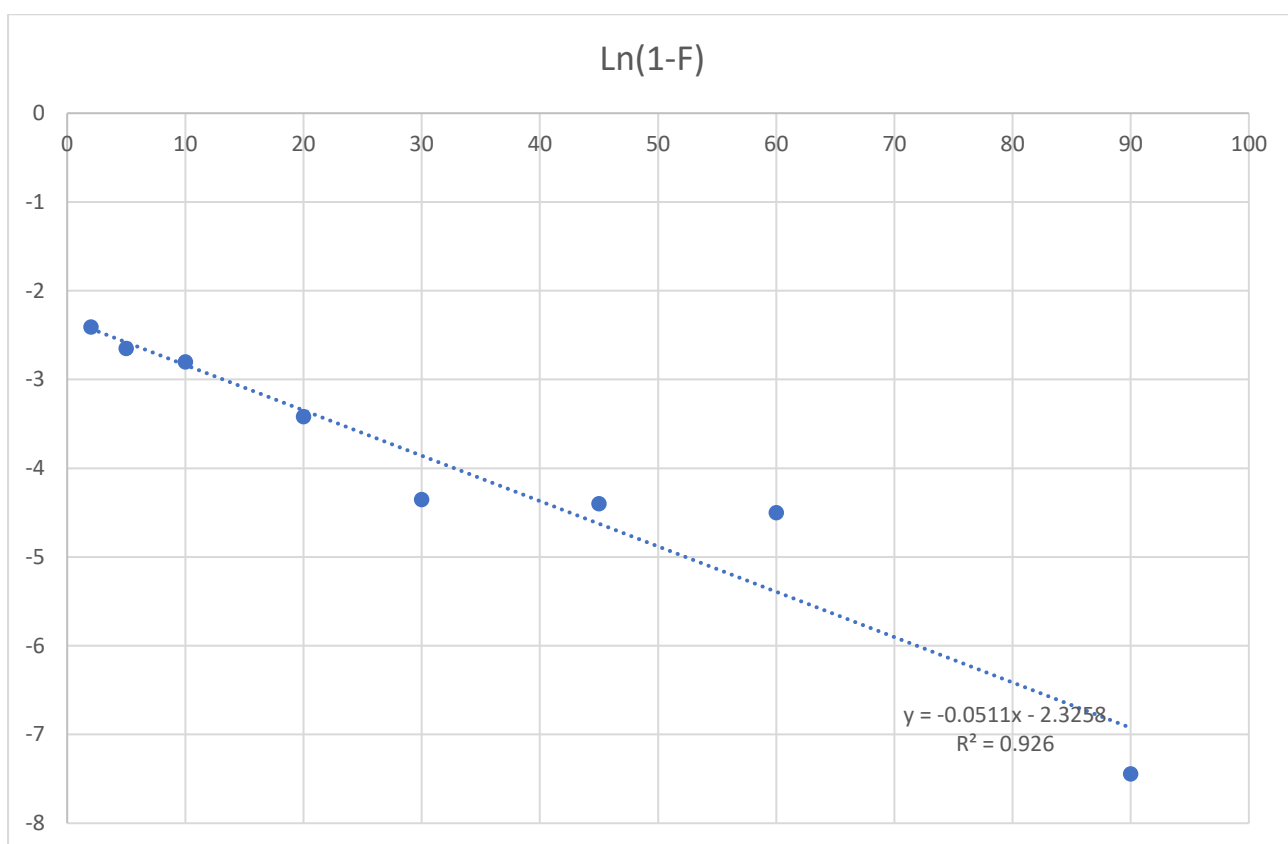Fig 7: LFDM for CIP adsorption by GCNPs.

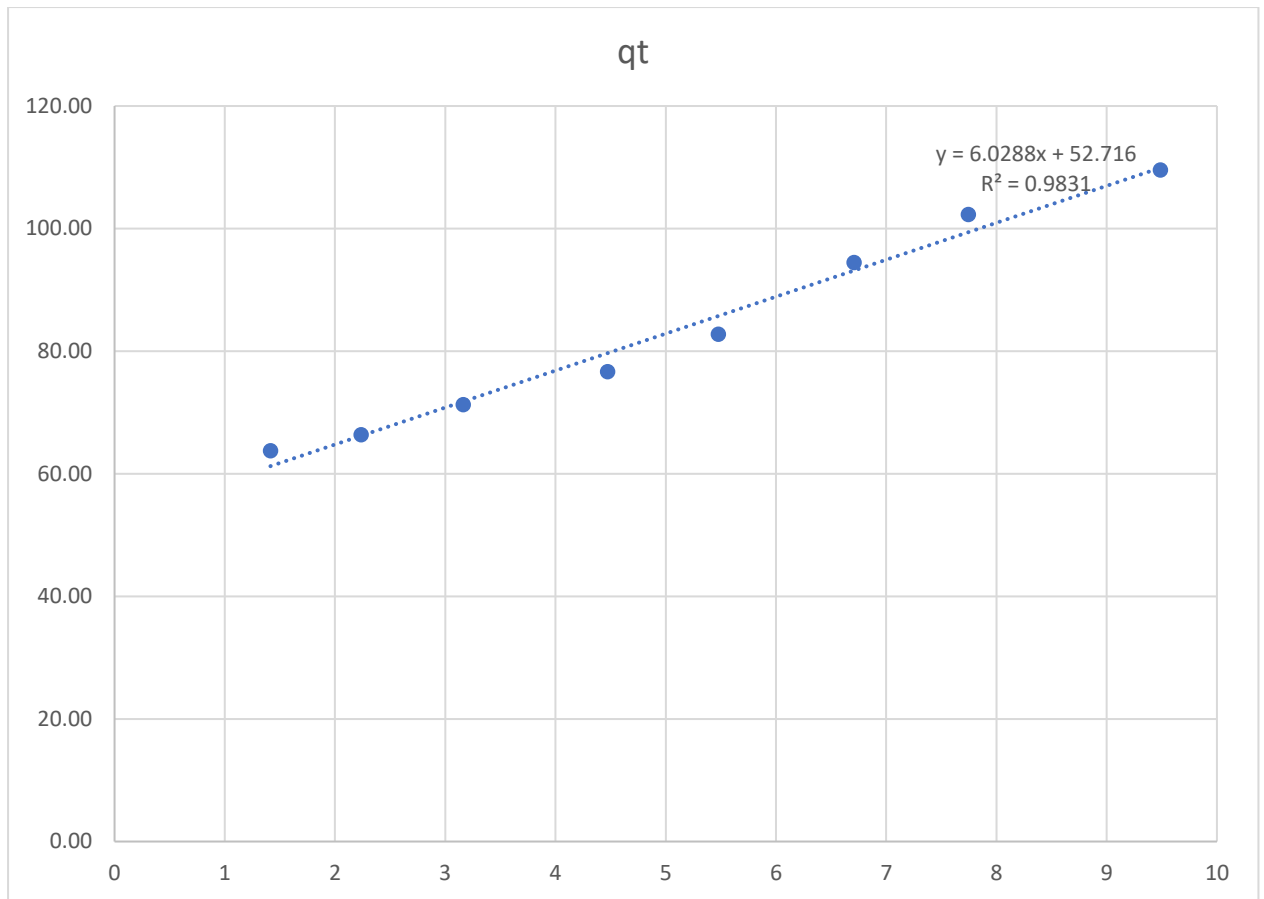Fig 8: LFDM for CIP adsorption by OCNPs.

Fig 9:   IPDM for CIP adsorption by GCNPs.

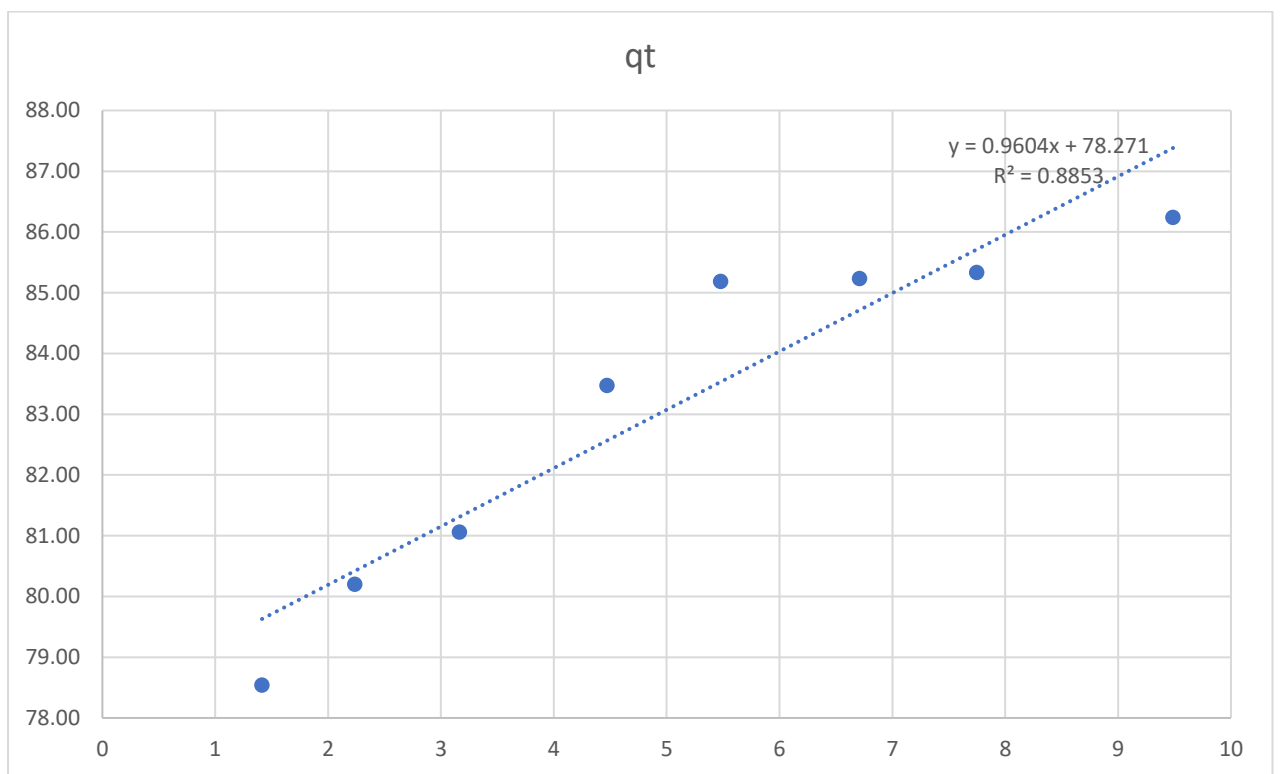Fig 10:   IPDM for CIP adsorption by OCNPs.

Table 3: The mechanism controlled the adsorption process

Sorbent	LFDM		IPDM	
	K_{LF} (min^{-1})	R^2	K_{IP} (mg g^{-1} min$^{0.5}$)	R^2
GCNP	0.0697	0. 859	15.82	0.98
OCNP	0.0751	0.926	13.70	0.885

3.4. Conclusion

The CCNP, OCNP and PCNP were employed to remove CFXN from water. The adsorption of the CFXN on PCNPs and CCNPs required 90 min to reach equilibrium. The maximum adsorption capacity values for CCNPs and PCNPs sorbents were found to be 114.8 mg g-1, and 90.7 mg g-1, respectively. Based on the study results, it was found that the adsorption kinetics of CFXN on CCNPs, and PCNPs followed the PSO. Furthermore, the adsorption rate control mechanism investigations revealed that IPDM controlled the CFXN adsorption on GCNPs, while LFDM controlled the sorption onto the PCNPs.

.

References

1. MISHRA, R., et al., *INVESTIGATION OVER WATER QUALITY OF RIVERS GANGA AND YAMUNA DURING KUMBH-2019-A CASE STUDY AT PRAYAGRAJ (ALLAHABAD), UTTAR PRADESH, INDIA.*
2. Yihdego, Z.J.B.R.P.i.I.W.L., *The fairness 'dilemma'in sharing the Nile waters: what lessons from the grand Ethiopian renaissance dam for international law?* 2017. **2**(2): p. 1-80.
3. Manahan, S., *Environmental chemistry.* 2017: CRC press.
4. Verma, J., et al., *Marine pollution, sources, effect and management.* Three Major Dimensions of Life: Environment, Agriculture and Health. Prayagraj, India: Society of Biological Sciences and Rural Development, 2020: p. 270-276.
5. Sjerps, R.M., et al., *Occurrence of pesticides in Dutch drinking water sources.* 2019. **235**: p. 510-518.
6. Hu, Y., et al., *Preliminary assessment of heavy metal contamination in surface water and sediments from Honghu Lake, East Central China.* 2012. **6**(1): p. 39-47.
7. Pan, Z., et al., *Environmental implications of microplastic pollution in the Northwestern Pacific Ocean.* 2019. **146**: p. 215-224.
8. Kurwadkar, S., S.R. Kanel, and A.J.W.E.R. Nakarmi, *Groundwater pollution: Occurrence, detection, and remediation of organic and inorganic pollutants.* 2020. **92**(10): p. 1659-1668.
9. Yadav, K.K., et al., *Fluoride contamination, health problems and remediation methods in Asian groundwater: A comprehensive review.* 2019. **182**: p. 109362.
10. Adimalla, N., J.J.H. Wu, and e.r.a.a.i. journal, *Groundwater quality and associated health risks in a semi-arid region of south India: Implication to sustainable groundwater management.* 2019. **25**(1-2): p. 191-216.
11. Salman, S.A., M. Arauzo, and A.A.J.G.f.S.D. Elnazer, *Groundwater quality and vulnerability assessment in west Luxor Governorate, Egypt.* 2019. **8**: p. 271-280.
12. Lee, H., et al., *Emergence and spread of cephalosporin-resistant Neisseria gonorrhoeae with mosaic penA alleles, South Korea, 2012–2017.* 2019. **25**(3): p. 416.
13. Villagomez, C., et al., *Self-assembly of enantiopure domains: The case of indigo on Cu (111).* The Journal of chemical physics, 2010. **132**(7): p. 074705.
14. Salama, A., et al., *Photocatalytic degradation of organic dyes using composite nanofibers under UV irradiation.* Applied Nanoscience, 2018. **8**(1): p. 155-161.
15. Hernández-Gordillo, A., et al., *Photodegradation of Indigo Carmine dye by CdS nanostructures under blue-light irradiation emitted by LEDs.* Catalysis Today, 2016. **266**: p. 27-35.
16. de Oliveira Brito, S.M., et al., *Brazil nut shells as a new biosorbent to remove methylene blue and indigo carmine from aqueous solutions.* Journal of Hazardous Materials, 2010. **174**(1-3): p. 84-92.
17. Gómez-Solís, C., et al., *Photodegradation of indigo carmine and methylene blue dyes in aqueous solution by SiC–TiO2 catalysts prepared by sol–gel.* Journal of hazardous materials, 2012. **217**: p. 194-199.
18. El Gaini, L., et al., *Removal of indigo carmine dye from water to Mg–Al–CO3-calcined layered double hydroxides.* Journal of Hazardous Materials, 2009. **161**(2-3): p. 627-632.
19. Yazdi, M.G., et al., *Surface modified composite nanofibers for the removal of indigo carmine dye from polluted water.* RSC advances, 2018. **8**(43): p. 24588-24598.
20. Secula, M.S., I. Creţescu, and S. Petrescu, *An experimental study of indigo carmine removal from aqueous solution by electrocoagulation.* Desalination, 2011. **277**(1-3): p. 227-235.
21. Lu, Y., et al., *The removal of Indigo Carmine from water by solvent sublation.* Seperation Science and Technology, 2005. **40**(5): p. 1115-1127.
22. Koltsov, I., et al., *Mechanism of reduced sintering temperature of Al2O3–ZrO2 nanocomposites obtained by microwave hydrothermal synthesis.* Materials, 2018. **11**(5): p. 829.

23. Hussein, M.A., et al., *Porous Al2O3-CNT nanocomposite membrane produced by spark plasma sintering with tailored microstructure and properties for water treatment.* Nanomaterials, 2020. **10**(5): p. 845.

24. Abdel-Naby, A.S., et al., *Synthesis, Characterization of Chitosan-Aluminum Oxide Nanocomposite for Green Synthesis of Annulated Imidazopyrazol Thione Derivatives.* Polymers, 2021. **13**(7): p. 1160.

25. Schubert, M., J. Exner, and R. Moos, *Influence of carrier gas composition on the stress of Al2O3 coatings prepared by the aerosol deposition method.* Materials, 2014. **7**(8): p. 5633-5642.

26. Seo, P.W., et al., *Adsorptive removal of pharmaceuticals and personal care products from water with functionalized metal-organic frameworks: remarkable adsorbents with hydrogen-bonding abilities.* Scientific reports, 2016. **6**: p. 34462.

27. Lima, E.C., *Removal of emerging contaminants from the environment by adsorption.* Ecotoxicology and environmental safety, 2018. **150**: p. 1-17.

28. Xu, Y., et al., *Advances in technologies for pharmaceuticals and personal care products removal.* Journal of Materials Chemistry A, 2017. **5**(24): p. 12001-12014.

29. Adeleye, A.S., et al., *Engineered nanomaterials for water treatment and remediation: costs, benefits, and applicability.* Chemical Engineering Journal, 2016. **286**: p. 640-662.

30. Jiang, J.-Q.J.C.O.i.C.E., *The role of coagulation in water treatment.* 2015. **8**: p. 36-44.

31. Teh, C.Y., et al., *Recent advancement of coagulation–flocculation and its application in wastewater treatment.* 2016. **55**(16): p. 4363-4389.

32. Cui, H., et al., *Application progress of enhanced coagulation in water treatment.* 2020. **10**(34): p. 20231-20244.

33. Goula, A.M., et al., *The effect of influent temperature variations in a sedimentation tank for potable water treatment—A computational fluid dynamics study.* 2008. **42**(13): p. 3405-3414.

34. Cheremisinoff, N.J.U.S.o.A., *Handbook of water and wastewater treatment technologies. Butterworth-Heinemann.* 2002.

35. Ratnayaka, D.D., M.J. Brandt, and M. Johnson, *Water supply.* 2009: Butterworth-Heinemann.

36. Gray, N., *Water technology.* 2017: CRC Press.

37. Kristiana, I., et al., *The formation of halogen-specific TOX from chlorination and chloramination of natural organic matter isolates.* 2009. **43**(17): p. 4177-4186.

38. Symons, J.M., *Factors affecting disinfection by-product formation during chloramination.* 1998: American Water Works Association.

39. Driedger, A.M., J.L. Rennecker, and B.J.J.W.R. Mariñas, *Sequential inactivation of Cryptosporidium parvum oocysts with ozone and free chlorine.* 2000. **34**(14): p. 3591-3597.

40. Venczel, L.J.A.E.M., *M, Arrowood, M. Hurd and MD Sobsey, Inactiva-tion of Cryptosporidium parvum Ocysts and Chstridium perfringens spores by a mixed-oxidant disinfectant and free chlorine.* 1997. **63**: p. 1598-1601.

41. Li, H., et al., *Comparative electrochemical degradation of phthalic acid esters using boron-doped diamond and Pt anodes.* 2010. **80**(8): p. 845-851.

42. Stara, J.F., D. Kello, and P.J.E.H.P. Durkin, *Human health hazards associated with chemical contamination of aquatic environment.* 1980. **34**: p. 145-158.

43. Bhanvase, B.A., et al., *Handbook of Nanomaterials for Wastewater Treatment: Fundamentals and Scale up Issues.* 2021: Elsevier.

44. Elamin, M.R., B.Y. Abdulkhair, and A.O. Elzupir, *Insight to aspirin sorption behavior on carbon nanotubes from aqueous solution: Thermodynamics, kinetics, influence of functionalization and solution parameters.* Scientific reports, 2019. **9**(1): p. 1-10.

45. Acharya, J., et al., *Removal of lead (II) from wastewater by activated carbon developed from Tamarind wood by zinc chloride activation.* Chemical Engineering Journal, 2009. **149**(1-3): p. 249-262.